Case Studies in Thermal Engineering 55 (2024) 104083

Contents lists available at ScienceDirect

Case Studies in Thermal Engineering

journal homepage: www.elsevier.com/locate/csite

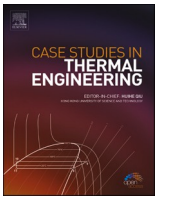

Optimum tilt and azimuth angles of heat pipe solar collector, an experimental approach

Donghui Wei [a,*], Ali Basem [b], As'ad Alizadeh [c], Dheyaa J. Jasim [d], Haydar A. S. Aljaafari [e,f], Mohammadali Fazilati [g,**], Babak Mehmandoust [g], Soheil Salahshour [h,i,j]

[a] College of Electrical and Information, Northeast Agricultural University, Harbin, HeiLongjiang, 150030, China
[b] Faculty of Engineering, Warith Al-Anbiyaa University, Karbala, 56001, Iraq
[c] Department of Civil Engineering, College of Engineering, Cihan University-Erbil, Erbil, Iraq
[d] Department of Petroleum Engineering, Al-Amarah University College, Maysan, Iraq
[e] Department of Chemical and Biochemical Engineering, 4133 Seamans Center for the Engineering Arts and Sciences, University of Iowa, Iowa City, IA, 52242, USA
[f] Department of Chemical Engineering, University of Technology, Baghdad, 10066, Iraq
[g] Department of Mechanical Engineering, Khomeinishahr Branch, Islamic Azad University, Khomeinishahr, Iran
[h] Faculty of Engineering and Natural Sciences, Istanbul Okan University, Istanbul, Turkey
[i] Faculty of Engineering and Natural Sciences, Bahcesehir University, Istanbul, Turkey
[j] Department of Computer Science and Mathematics, Lebanese American University, Beirut, Lebanon

ARTICLE INFO

Keywords:
Heat pipe solar collector
Optimum tilt angle
Azimuth angle
Anisotropic sky radiation model

ABSTRACT

The application of solar energy as the widest, clean and free source of thermal energy requires the solar collector. As one of the common types of solar collector, heat pipe solar collector has been investigated. The thermal performance of a solar heat pipe collector was simulated using the anisotropic sky radiation model in eight different tilt angles and thirteen azimuth angles at the location of Isfahan City, Iran. The obtained theoretical results were compared with experimental ones and an average discrepancy of 5 % was obtained. After approving the chosen model, the optimum seasonal and yearly tilt angles were calculated and the correlations also were drawn from a written subroutine. The results show that through spring and summer, the optimum tilt angle is somewhat less and through autumn and winter the optimum tilt angle is beyond the latitude angle with the largest difference in spring and autumn. For the whole year and under the conditions of the present study, the optimum tilt angle is nearly the same as the latitude angle of the location.

Abbreviations

3 dimensional	*3D*
Collector surface area (m^2)	*A*
specific heat (kJ/kg.K)	*cp*

* Corresponding author.
** Corresponding author.
E-mail addresses: weidonghui0895@sina.com (D. Wei), asad.alizadeh2010@gmail.com (A. Alizadeh), Fazililati@iaukhsh.ac.ir (M. Fazilati).

https://doi.org/10.1016/j.csite.2024.104083
Received 18 December 2023; Received in revised form 20 January 2024; Accepted 29 January 2024
Available online 3 February 2024

Solar radiation flux (W/m^2) G
Heat pipe HP
global horizontal solar irradiation I
sky clearance index KT
mass (kg) m
day number n
Photovoltaic/thermal PV/T
absorbed heat (kJ) Q
Radiation flux (W/m^2) R
geometric coefficient Rb
temperature (^{o}C) T
time (minute) t

Greek symbols
collector tilt angle β
difference Δ
surface azimuth angle γ
latitude angle φ
reflectivity ρ
regular incident angle θ
incident angle with $\beta = 0$ θ_z

Subscripts
air A
direct components of input radiation b
diffuse components of input radiation d
ground g
mass (kg) m
normal component n
outside o
optimum opt
Solar constant sc
total T

1. Introduction

By the growth of technology, the human lifestyle and the societies and the civilization the use of energy increased dramatically [1]. The major part of this need is met by traditional sources such as gas, oil, and petroleum and fossil fuels account for more than 80 % of total energy consumption. The depletion of fossil based energy sources and their environment issues are the main derivations for implementing different sustainable energy resources. Among renewable energy sources and by its great potential such as availability and environment friendly, solar energy achieves the first rank. The Incident solar energy on the Earth is more than 200 times greater than the annual total commercial power currently consumed by humans [2]. The direct application of solar energy could be made in two forms solar thermal and solar electricity via the application of solar photovoltaic (*PV*) and collector panels, respectively. The solar collector is a type of heat exchanger that absorbs the incoming solar radiation and then, transforms the absorbed heat to the working fluid. Depending on the type of application, the augmented heat could be used directly or stored in storage systems for later usage [3–5]. As the main component of the system the performance of solar thermal systems is greatly affected by the design and operation characteristics of the solar collectors [6]. Flat plate, evacuated tube and heat pipe and photovoltaic/thermal (*PV/T*) [7] solar collectors are the most popular types of solar collectors and their thermal performance has been investigated in different working conditions. In every type of solar collector, the target is to catch the maximum possible solar irradiance or solar energy on the collector's surface area. Through different experimental [8] and numerical [9] works, it has been argued that between different parameters, the inclination angle has a major effect on the performance of solar collectors. The best installation angle of the solar collector depends on the local latitude and the sun tracking systems provide the normal-to-radiation situation. Elnaggar [10] employed the solar collector for the purpose of water and space heating in Gaza strip and found the best inclination angle of 30 and 45° for the corresponding solar collectors, respectively. In other work, he and coauthors [11] simulated the performance of a solar hot water system and found the optimum tilt. They reported the dependency of useful energy gain of on the values of the tilt and incidence angles; the best angles is not fixed all over the year instead it has different values that are subject to the season or months of the year. The sun-tracking systems yield the highest solar energy efficiency. Through the state-of-art review on tracking systems, Mousazadeh et al. [12] found that by using the sun tracker, the collected solar energy could be increased by 10–100 % depending on the period of the year. Compared to the fixed system, Abdallah [13] reported a 43.87 % higher daily energy collection for the solar tracking system. By their relatively higher price,

the solar tracking systems are employed less frequently and not recommended, particularly for using in small solar panels [12,14]. Instead and as the replacement, the optimum tilt angle installation has the advantage of not-involving tracking cost expenditure. Through a numerical simulation, Despotovic et al. [15] demonstrated that compared to fixed-angle-mounted *PV* panels in Belgrade, the annual yearly, seasonal and monthly energy yield for the panels positioned at optimum tilt angles increased by 5.98 %, 13.55 % and 15.42 %, respectively. By changing the solar collectors' tilt angle from the fixed value to the optimum one, Skeiker [16] found that a gain of 30 % could be obtained. In Tabass city of Iran, by adjusting the tilt angle of *PV* panels to the optimum angle, the monthly, seasonal, semi-yearly and yearly gain has been increased by 23.15 %, 21.55 %, 21.23 % and 13.76 %, respectively [17]. Sharma et al. [18] investigated tilt angles for different months in Hamirpur, Himachal Pradesh, India. Several models were used to estimate the monthly optimum tilt angles for this site. It was found that the M − 11 model, with three annual adjustments, estimates better than the other models.

A heat pipe solar collector is a two-phase heat exchanger system. The *HP* solar collector with advantages over the other types of solar collector including high overall efficiency, high heat transfer capability, resistance to freezing and low heat losses, no overheating and fast start and resistance to high pressure and thermal shock, making them a suitable candidate for solar thermal systems [19]. The performance of *HP* systems is affected by different parameters including the geometry, working fluid, filling ratio and inclination angle [20]. Like the other types of solar collectors, the yield performance of the *HP* systems is the function of the tilt angle and orientation. The optimum inclination angle of the *HP* for achieving the better heat transfer is usually not the same that for achieving the maximum solar irradiation. The increasing and decreasing effect of the inclination angle on collector efficiency was reported by Hassan and Hussein [21]. In this way, they demonstrated, for choosing the optimum inclination angle the effects of both heat transfer and solar irradiance absorption should also be considered. Zhang et al. [21] investigated the performance of a photovoltaic/thermal (*PV/T*) system in different tilt angles using a *3D* numerical and experimental approach. The results demonstrated that the thickness of the liquid film in the evaporator and condenser stabilizes at inclining conditions. Eventually, the obtained numerical and experimental results demonstrated that the optimum inclination angle is 40^{o}. Hu et al. [22] compared the performance of the wickless and wire meshed *HP* in a *PV/T* solar system at different tilt angles under the same climate and solar conditions. They reported the higher sensitivity of the wickless *HP* than the wire-meshed collector to changing the inclination angle. They also recommended the wire meshed *HP* for latitudes less than 20° and the wickless *HP* systems for higher latitudes.

Considering the wide application of the heat pipe collector in solar thermal systems, improving the thermal efficiency of these systems is a main goal. The highest solar radiation absorption would be naturally at a normal angle but it is usually not practical to track the sun. Therefore, finding the best orientation for the achievement of the highest thermal efficiency is inevitable. Many studies proposed various schemes for determining the optimum tilt angle for the solar collector's installation in different latitudes [23,24]. Despite the efforts made for the estimation of optimum tilt angles, no definite value or method was accepted universally and the proposed optimum angles for the same latitude differ for more than 15° [25], 10° [26] and $\pm 10^{o}$ [27]. The literature review made by the authors revealed that the experimental paralleled with theoretical study of *HP* collectors in country of Iran has not received much attention. In this work, the optimum tilt angles of *HP* solar collectors in Isfahan, Iran investigated. The optimum tilt and surface azimuth angles are found for the investigated *HP* collector. Eight different tilts and thirteen different azimuth angles were investigated. The work approach is theoretical which validated and optimized against the experimental result. The anisotropic sky model was chosen for modeling the performance of the evacuated *HP* tube which is located in Isfahan city (63.2^{o} Northern latitude) and its accuracy verified against the experiment. The optimum orientation angle was then determined based on the employed model and finally the correlations derived for different installation angles.

2. The theoretical background

For the estimation of global solar radiation on horizontal surfaces different models could be implemented. These models use the climatic parameters as the inputs including sunshine duration, wind, humidity and temperatures conditions [28] and give the beam and diffuse solar radiation incident on a horizontal surface. By determining these factors, the radiation over tilted surfaces could also be driven which used to overcast the performances of tilted solar collectors. Total radiation incident on a tilted surface consists of three components: beam radiation, diffuse radiation and ground reflected radiation. The beam component could be determined using a simple relationship; moreover, the ground reflected radiation can be estimated using the isotropic model, but this is not the case for the diffuse component, by the fact that diffuse radiation has no unique angle of incidence. There are various models which correlate the diffuse radiation on a tilted surface to that on a horizontal surface and could be classified as isotropic and anisotropic sky models. Based on isotropic models the radiation intensity is uniform over the sky. In this way, the incident diffuse radiation on the inclined surface is dependent on the fraction of sky dome seen by it. However, the anisotropic models deal the sky radiation as an aisotrpic diffuse radiation in the circumsolar region and the isotropic component from the rest of the sky dome [29]. In general, the diffused component of radiation on tilted surfaces is the combination of isotropic, circumsolar and horizon brightening parts.

The hourly total radiation to the tilted surface located at the declination angle of β could be determined using the Hay model, as given by Eq. (1) [25] which also validated experimentally [30,31];

$$I_T = (I_b + I_d A_i) R_b + I_d (1 - A_i) \left(\frac{1 + \cos \beta}{2} \right) + I \rho_g \left(\frac{1 - \cos \beta}{2} \right) \tag{1}$$

in Eq. (1), I and R_b represent the global horizontal solar irradiation and geometric coefficient, and subscripts b and d denote the direct and diffuse components of input radiation, respectively; also, ρ_g is the ground reflectivity or Albedo coefficient [32]. The diffuse radiation portion is determined according to Erbs [33] by experimentally validated Eq. (2) [30,31];

$$\frac{I_d}{I}=\begin{cases}1-0.09K_T & for\ K_T\le 0.22\\ 0.9511-0.1604K_T+4.388K_T^2-16.683K_T^3+12.336K_T^4 & for\ 0.22\le K_T\le 0.8\\ 0.165\ for\ K_T>0.8\end{cases} \tag{2}$$

The parameter K_T in Eq. (2) is the sky clearance index whose value depends on the latitude of location and the month, as listed in Table 1 [30,31]. To determine the diffuse radiation, it is necessary to have the value of clear sky irradiation, (I) which is determined by Eq. (3).

$$K_T=\frac{I}{I_o} \tag{3}$$

The parameter "I_o" in Eq. (3) is the outside-atmosphere solar radiation which is calculated according to Eq. (4) [34];

$$I_O=\frac{12\times 3600G_{SC}}{\pi}\left(1+0.033\ cos\frac{360n}{365}\right)\times\left(cos\ \delta\times\cos\varphi\times(sin\ \omega_2-sin\ \omega_1)+\frac{\pi(\omega_2-\omega_1)}{180}sin\ \varphi\ sin\ \delta\right) \tag{4}$$

In Eq. (4) φ is the latitude which is 32.6° and G_{sc} is the solar constant whose value is 1367 W/m^2. The parameter n demonstrates the day of the experiment. The δ angle is determined considering the day number (n) according to Eq. (5) [35].

$$\delta=23.45\ \sin\left(360\frac{284+n}{365}\right) \tag{5}$$

The value of (ω_1) in Eq. (4) for two-time intervals of 10:30 to 12 and 11:30 to 12 is −2.5 and −7.5, respectively. Considering the time interval of data acquisition wiz 5 min, the time angle of (ω_2) is obtained by adding ($\frac{5}{60}$) to ω_1. The solar beam radiation (I_b in Eq. (1)) is determined by subtracting the diffuse radiation (Eq. (2)) from total radiation (Eq. (3));

$$I_b=I-I_d \tag{6}$$

The Albedo coefficient, ρ_g in Eq. (1), represents the reflective coefficient of the surrounding surface and its value depends on the type of surface around the collector [25]; considering the ground-type mosaic flooring, the value of 0.2 taken for the magnitude of albedo coefficient [36]. The geometric coefficient denotes the direct radiation on an inclined surface to that on the horizontal surface and is given by Eq. (7).

$$R_b=\frac{\cos\theta}{\cos\theta_Z} \tag{7}$$

The parameters θ and θ_z in Eq. (7) are the regular incident angle and incident angle with β = 0 (Eq (9) and (10), respectively).

$$\cos\theta=(\sin\delta\times\sin\varphi\times\cos\beta)-(\sin\delta\times\cos\varphi\times\sin\beta\times\cos\gamma)+(\cos\delta\times\cos\varphi\times\cos\beta\times\cos\omega)$$
$$+(\cos\delta\times\sin\varphi\times\sin\beta\times\cos\gamma\times\cos\omega)+(\cos\delta\times\sin\beta\times\sin\gamma\times\sin\omega) \tag{9}$$

$$\cos\theta_Z=(\sin\delta\times\sin\varphi)+(\cos\delta\times\cos\varphi\times\cos\omega) \tag{10}$$

The parameter A_i in Eq. (1) is determined using Eq. (11) having I_b and I_o (from Eq. (7) and Eq. (4), respectively).

$$\frac{I_{bn}}{I_{on}}=\frac{I_b}{I_o} \tag{11}$$

The solar irradiance received to the collector surface is obtained by multiplying the total solar radiation (I_T in Eq. (1)) by the collector absorbing area. If the solar ray with the intensity of I_b incident to the collector surface, the energy absorbed by the infinitesimal normal area of dA_n could be obtained by Eq. (12).

$$dQ_b=dA_n.I_b\ \rightarrow\ \int dQ_b=\int dA_n.I_b\ \rightarrow\ Q_b=A_n.I_b \tag{12}$$

Considering that always half of the tube surface is posed directly to solar radiation (Fig. 1) the differential area of dA_n and the collector normal surface (A_n) is determined using Eq. (13).

$$dA_n=L\times\frac{D}{2}\times d\lambda\ \rightarrow\ A_n=L\times\frac{D}{2}\int_{-\frac{\pi}{2}}^{\frac{\pi}{2}}d\lambda=L\frac{D}{2}\pi \tag{13}$$

The total incident radiation could also be determined in a similar approach as specified in Eq. (14)

Table 1
The values of the sky clearance index for different months and latitude of 36.2°

Jan	Feb	Mar	Apr	May	June	July	Aug	Sep	Oct	Nov	Dec
0.49	0.51	0.48	0.49	0.53	0.58	0.56	0.56	0.58	0.55	0.51	0.51

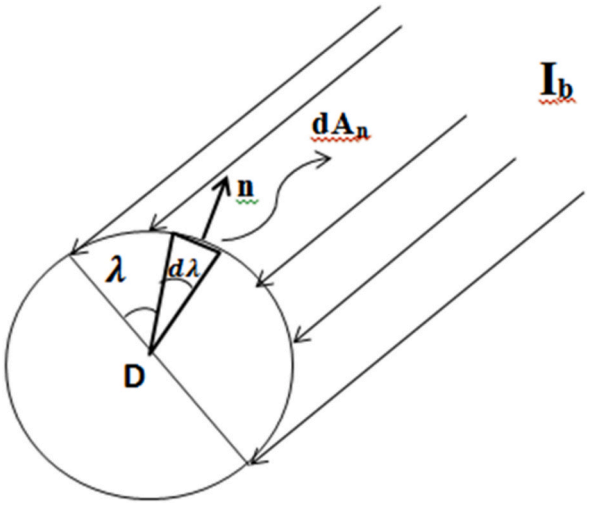

Fig. 1. The incident direct beam to evacuated *HP* and the differential absorbing area.

$$dQ_T = dA_n.I_T \rightarrow \int dQ_T = \int dA_n.I_T \rightarrow Q_T = A_n.I_T \tag{13}$$

The absorbed solar radiation would increase the water temperature by the value of ΔT (Eq. (14)), where the parameters Q_T, m and c are the absorbed solar radiation (kJ), the mass of water (kg) and specific heat capacity of water, respectively;

$$Q_T = mc\Delta T \tag{14}$$

3. System description and methodology

The main component of the experimental setup is the evacuated heat pipe as shown in Fig. 1. The *HP* consists of two parts of the inner copper tube and the outer evacuated glass tube. The *HP* is a wickless type whose length and outer diameter are 1800 mm and 430 mm, respectively.

To study the effect of inclination angle on the thermal performance of the system, the *HP* tubes are installed at specific angles using the structure whose schematic and dimensions are depicted in Figs. 2 and 3. Also, to measure the heat absorption capacity of the tubes, the well-insulated container of 1 L is connected to the top of the tubes where the copper tube of *HP* is inserted there (Fig. 4). The thermal insulation is of polyethylene foam of 1.5 cm thickness which was wound around the container's outer surface. Also, to measure the instant temperature of the water the pre-calibrated glass thermometer is located inside the tank.

The experiments are organized in two separate groups; in the first stage, the beta angle (the inclination angle from the horizontal surface) is the input parameter which varied between 10 and 80°, and at the second stage, the effect of azimuth angle between −90 (east direction) to +90° (west direction) was examined. The test time is on 21 December (11 January) and the measurement time is in time intervals of 10:30 to 11:30 and 11:30 to 12:30 (symmetrical to solar noon); the quantities got and recorded every 5 min. To reveal the effect of the collector angle, the tests of different angles should be performed under the same solar and weather conditions. Therefore, for investigation the tilt angle effect, eight *HP* tubes and for the azimuth angle study 13 tubes were used as shown in Figs. 5 and 6, respectively. The water container of 1-L capacity is attached at the top of the tubes where the copper part of the *HP* tube is inserted. To increase the accuracy of measurements, all tubes are covered against the sun before beginning the tests. By triggering the

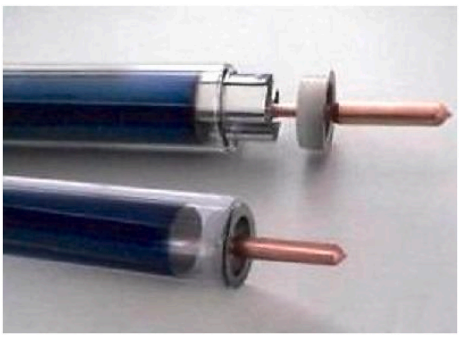

Fig. 2. The employed evacuated *HP* in the experiments.

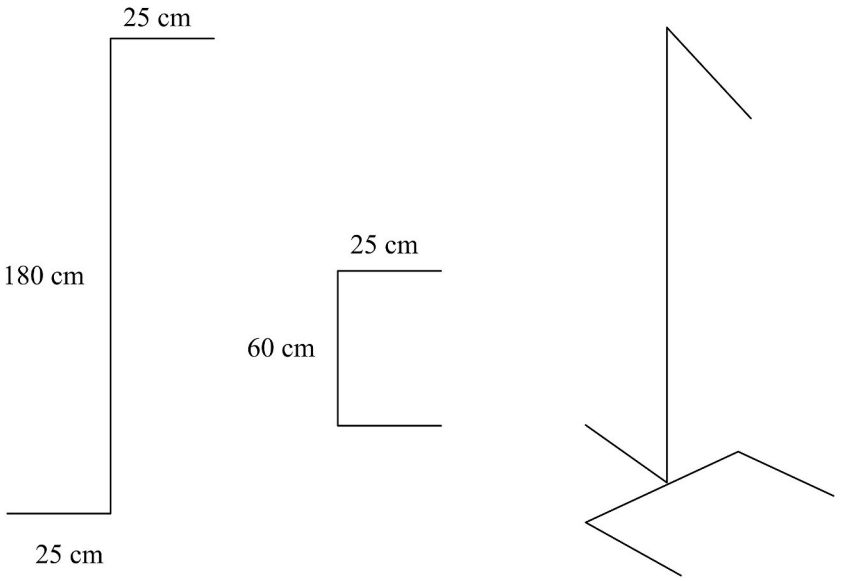

Fig. 3. The schematic and dimensions of the employed structure for installing the *HP* collector.

Fig. 4. The installation of a thermally insulated container above the *HP* tube.

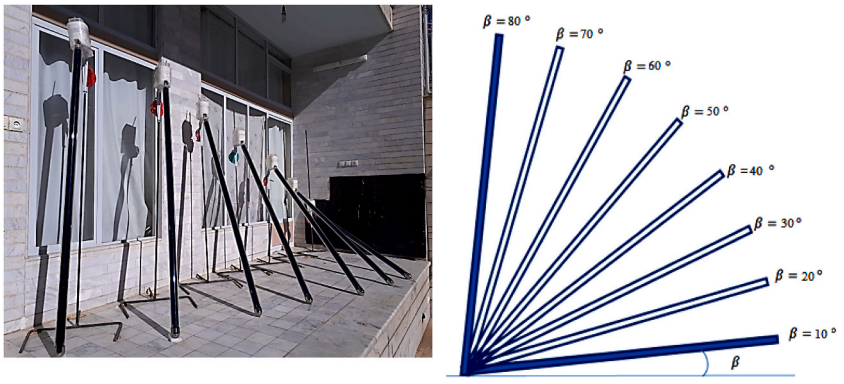

Fig. 5. The experiment rig for tilt angle study, left: photographic view, right: collector positions from the top view.

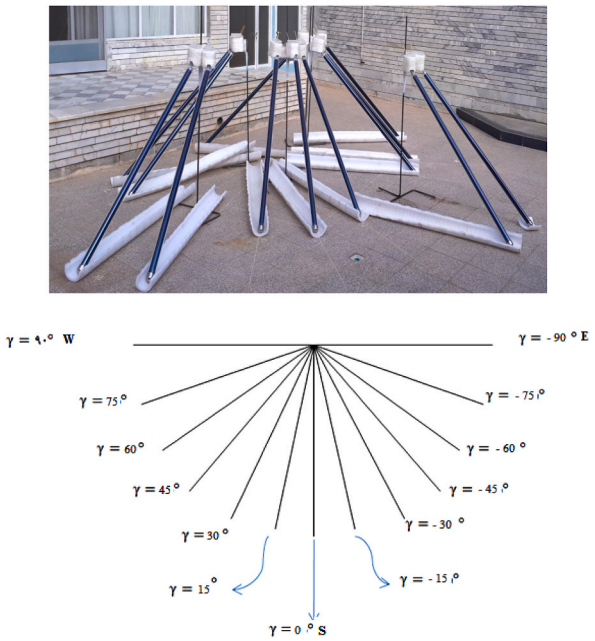

Fig. 6. The test rig for examining the surface azimuth angle, top: a photographic view, bottom: the position angles.

tests, the covers were removed simultaneously and the data acquisition begins by getting the temperatures every 5 min. The initial water temperature inside the tanks is 26 °C and the location of experiments is at the city of Isfahan.

The geographical location of the Isfahan City lies within North Latitude 23°6′, East Longitude 51°3′ and Altitude 1575 m at sea level. The location of Isfahan is in the central portion of Iran (Fig. 7).

The climate of Isfahan is temperate with hot and dry summer and cool winter. The average maximum and minimum yearly temperatures are 37 °C, and −7 °C, respectively. The total rainfall of the city is averagely 150 mm with the yearly relative humidity of about 40 %. The average horizontal solar radiation during the cold and hot periods of year is 15.9 and 27.4 MJ/m^2. The monthly average total radiation and air temperature for the study location listed in Table 2 [31].

3.1. The uncertainty study

The uncertainty analysis is an important part of the experimental studies. In the present work, the independent parameters are the tilt and surface azimuth angles and the dependent variable is the temperature. The uncertainty of the employed parameters along with their range is shown in Table 3. The uncertainty values listed in Table 3 is in fact the sensitivity of the measuring devices divided by the minimum value of the corresponding parameter recorded through the experiments.

3.2. Assumption, limitations and uncertainties of the results

The current work include two parts of experimental and theoretical sections; at first part the measuring process does not include any assumption and the results may be applied at similar weather and climate conditions within the uncertainty of measuring devices (as denoted in Table 2). For second part, the anisotropic sky radiation model could be employed for any weather conditions [29]; also,

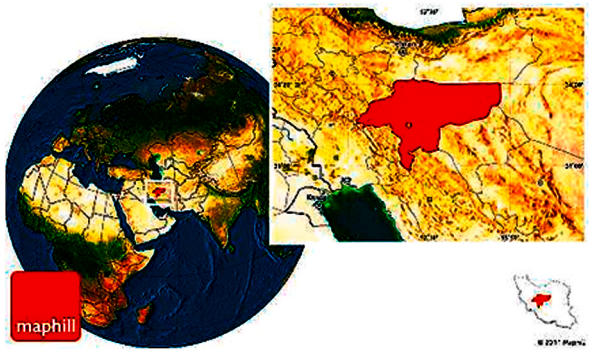

Fig. 7. Location map of Isfahan city and Isfahan province in country of Iran.

Table 2
The values of monthly average temperature and solar radiation for different months.

	Jan	Feb	Mar	Apr	May	June	July	Aug	Sep	Oct	Nov	Dec
I_T (MJ/m^2)	13.4	19.01	19.86	21.58	26.25	30.06	29.92	28.97	25.71	30.35	16.8	13.6
T_A	3.4	6.2	10.7	16	21.1	26.5	29	27.4	23.3	17	10.1	5

Table 3
The values of maximum, minimum, and maximum uncertainty of involved parameters in this study.

Parameter	Minimum	Maximum	Max. Uncertainty (%)
Tilt angle (β)	10	80	10 %
Azimuth angle (γ)	12.3	33.2	6.7
Temperature (T)	0.24	0.71	2.3

the correctness of the model has been verified by comparing its results with the experimental ones. In other words, one of the aims of this study is the verification of using this model for the analysis of *HP* solar collectors.

4. Results and discussion

The results are presented for two experimental schedules; the effect of varying the tilt angle and the orientation angle on heat absorption of the *HP*s investigated separately by inspecting the time variation of hot water temperature. For comparison, in each case, both the experimental and theoretical results were presented inside one diagram and the accuracy of the given model was examined. After validating the model, the optimum orientation and tilt angles are extracted and the correlations are drawn.

4.1. The effect of tilt angle

The effect of tilt angle on system performance has been investigated by exposing the heat pipe at different tilt angles against the sun and studying the time variation of stored hot water temperature. The investigated tilt angles are 10–80° with the interval of 10°; the temperature history of water for the investigated tilt angles at two consecutive time intervals are shown in Figs. 8–18. It is worth noting that in this stage, the heat pipe tubes are all positioned toward the south direction ($\gamma = 0$) and also, the water temperature at different times is determined via both experimental and theoretical approaches. By inspecting the variation of water temperature, an increasing trend could be observed for all tilt angles. In the first stage of the experiments, the temperature increased with a higher inclination rate than in the second stage, which is the result of the initial lower temperature of the water and the resulting higher heat transfer rate. Although this trend is seen for all tilt angle, the inclination rates is higher at higher tilt angles; the temperature increase at the second-time stage (from 60 to 77 min) is 5 °C and 22 °C in the case of 10 and 30° tilt angles, respectively. This behavior goes on until a tilt angle of 30°; by increasing the tilt angle from 30, the temperature inclination rate decreased again; for tilt angles of 50 and 80°, the temperature increase is 19 and 16 °C, respectively. This behavior which could also be seen in the first stage shows that there is an optimum tilt angle for which the system has the best performance. In other words, there is an optimum tilt angle for which the time rate of temperature increase is the highest.

By comparing the values of water temperature obtained from the experimental and theoretical approaches some level of deviation could be observed. The discrepancy between the measurement and theory is not the same at different tilt angles and two-time intervals. In the first part of the experiment (first time interval) and for tilt angles below 20° (i.e. tilt angles of 10° and 20°), the experimental values are higher than theoretical ones and for tilt angles of 30 and above, the reverse trend prevails. In the second time interval and for tilt angles of 10 and 20, a specific common trend could not be distinguished but, for tilt angles of 30 and more, the experimental results

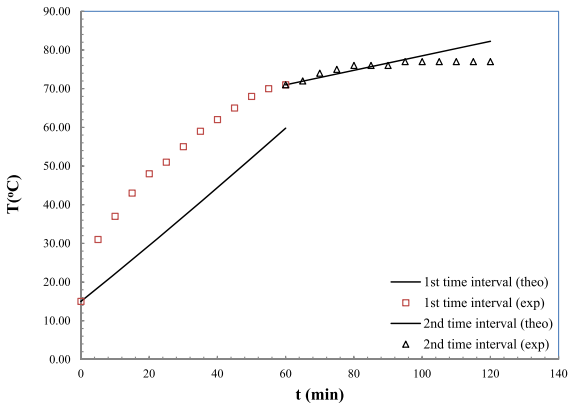

Fig. 8. The time variation of water temperature at tilt angle of 10° in two consecutive time intervals.

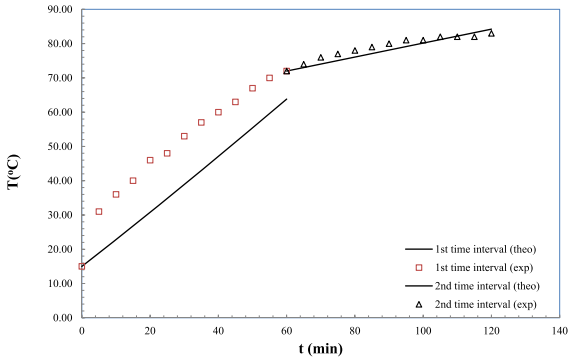

Fig. 9. The time variation of water temperature at a tilt angle of 20° in two consecutive time intervals.

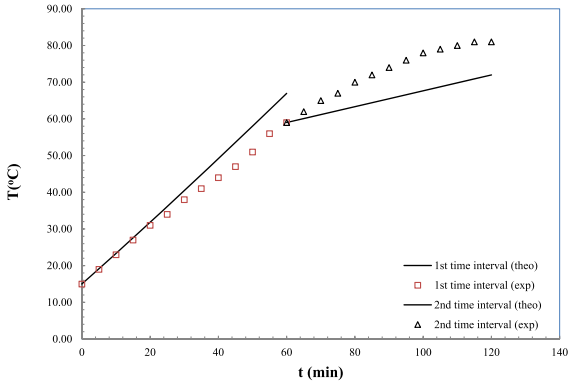

Fig. 10. The time variation of water temperature at tilt angle of 30° in two consecutive time intervals.

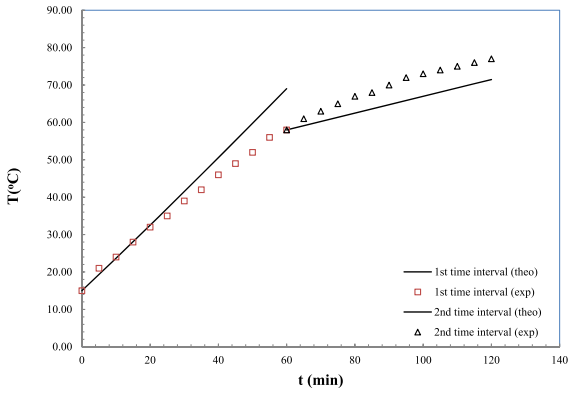

Fig. 11. The time variation of water temperature at a tilt angle of 40° in two consecutive time intervals.

are higher than the theoretical ones in all cases. The average difference between the experimental and theoretical results for different tilt angles at first and second-time intervals are shown in Figs. 14 and 15, respectively.

Despite the observed discrepancy between hot water temperatures obtained by the experiment and theory, the same variation patterns of the two approaches show the good accuracy of the anisotropic sky model for estimating the thermal performance of heat pipe collectors. The difference between the average water temperature obtained from the theoretical and experimental results for different tilt angles, as illustrated in Figs. 14 and 15 shows that there is no full match between the theory and experiment and also, the discrepancy differs for different tilt angles. The lower water temperatures of the experimental than the theoretical approach comes from the tube's heat loss to surroundings which has not been considered in calculations; this case is seen at higher-than-30° tilt angles and first-time intervals; at these tilt angles, the incident radiation to collector surface is so high that results to relatively high water

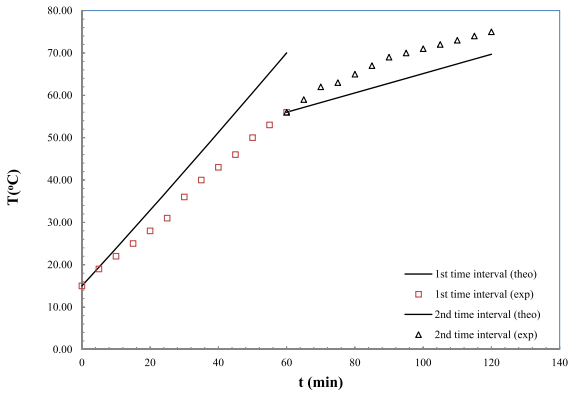

Fig. 12. The time variation of water temperature at tilt angle of 50° in two consecutive time intervals.

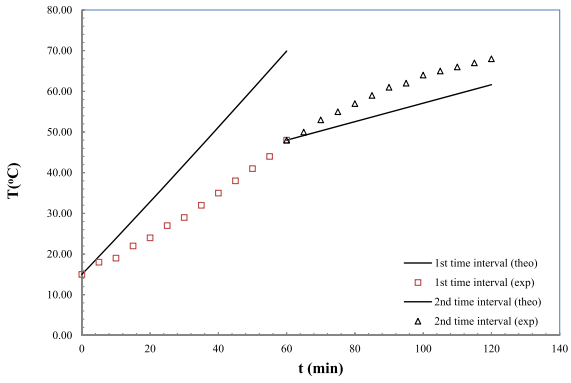

Fig. 13. The time variation of water temperature at tilt angle of 60° in two consecutive time intervals.

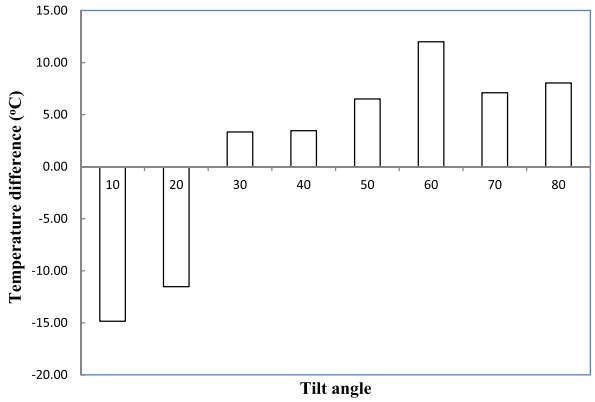

Fig. 14. The water temperature difference obtained from theory and experiment averaged between sampling times for different tilt angles at first-time interval.

temperature which increases the heat loss to surroundings. At the second time interval, the observed discrepancy is not so much and is within the uncertainty of measurements. The percent difference between the experimental and theoretical results in this time interval is depicted in Fig. 16; in this time interval, the difference between theoretical and experimental results averaged between different tilt angles is 5 %. Another factor which could be stated as the reason of discrepancy between the experimental and theoretical results is the assumption of direct radiation to *HP* and getting the half of collector surface area for determining the absorbed radiation (Fig. 1); by the existence of both diffuse and ground reflected radiation in addition to direct radiation and their simultaneous effect on the absorbed radiation, this unavoidable assumption would lead to some degree of error. And finally the difference between the inner glass and copper tubes which absorb and transfer the absorbed heat to the water, respectively and has not considered in calculations.

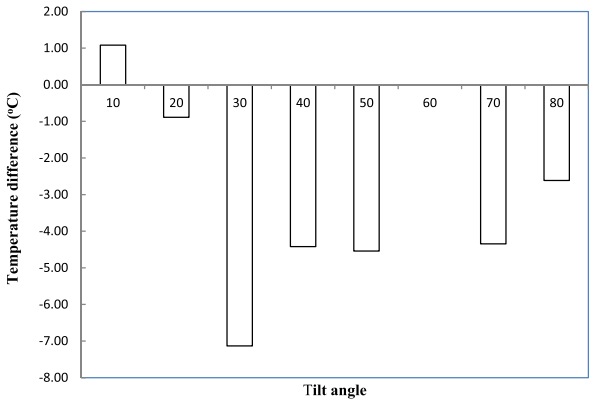

Fig. 15. The water temperature difference obtained from theory and experiment averaged between sampling times for different tilt angles at the second-time interval.

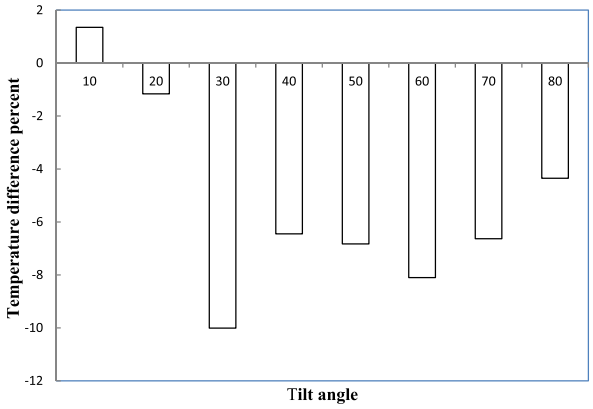

Fig. 16. The water temperature difference percent between theory and experiment averaged between sampling times for different tilt angles at second time interval.

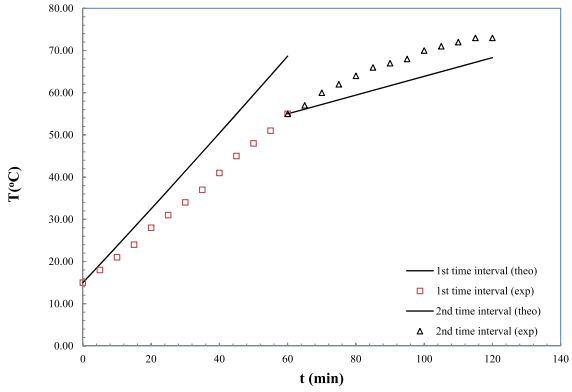

Fig. 17. The time variation of water temperature at a tilt angle of 70° in two consecutive time intervals.

4.2. The effect of surface azimuth angle

The effect of changing the surface azimuth angle has been studied by installing the heat pipes at different azimuth angles; in these cases, the fixed tilt angle of 45° was considered (Fig. 6). It is worth noting that the local south direction has been determined previously. The water temperature in cases of different azimuth angles of positive (west direction) and negative (east direction) angles is shown in Figs. 19–30; for the sake of better comparison, the diagrams of positive and negative angles are shown in sequence for each angle. By inspecting the figures, despite the ever-increasing of water temperature vs the time for all angles and at two-time intervals, the inclination rate is different at different angles. The percent change of water temperature during the 1st and 2nd time intervals for negative (East direction) and positive (West direction) are listed in Table 3.

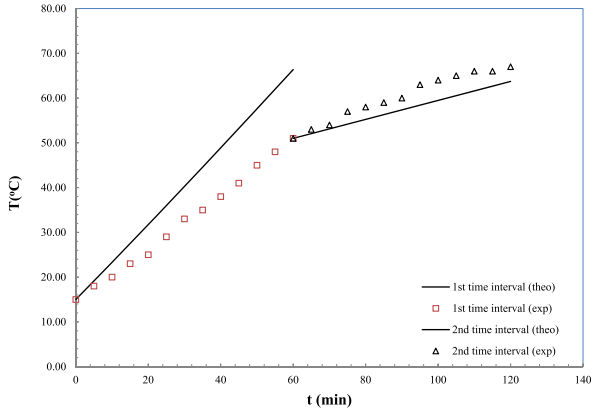

Fig. 18. The time variation of water temperature at tilt angle of 80° in two consecutive time intervals.

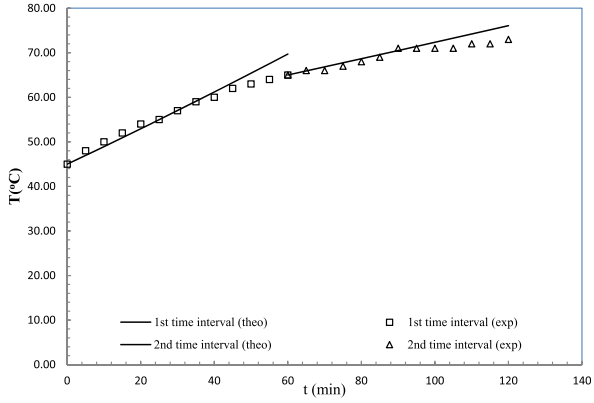

Fig. 19. The time variation of water temperature at azimuth angle of 15° in two consecutive time intervals.

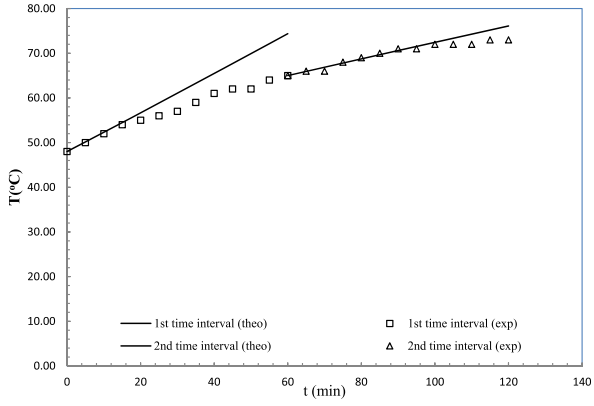

Fig. 20. The time variation of water temperature at an azimuth angle of −15° in two consecutive time intervals.

By inspecting the percent change of water temperature in different angles, the higher temperature increment during the first time interval could be observed; at an azimuth angle of −45°, the values of temperature percent change are 46 % and 3.3 % during the first and second time intervals. The higher temperature change during the first than second-time interval could be attributed to the relatively initial lower temperature of water which enhances the heat transfer absorption rate and results in higher temperature change at this period. Moreover, although the water temperature increment rate is higher during the first time interval at all azimuth angles, the difference between the temperature increment rate in the first and second time intervals is the highest at an angle of 45°. The difference in behavior of water temperature change for azimuth angle of 45° could be is the result of lower temperature increase during second time interval which is also the lowest between the other cases.

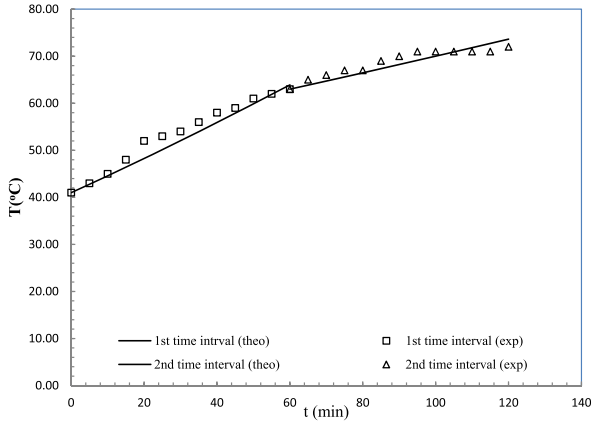

Fig. 21. The time variation of water temperature at azimuth angle of 30° in two consecutive time intervals.

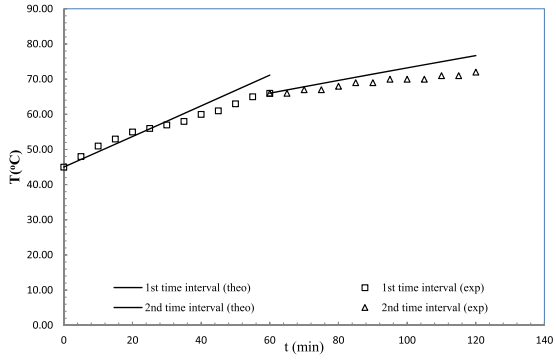

Fig. 22. The time variation of water temperature at an azimuth angle of −30° in two consecutive time intervals.

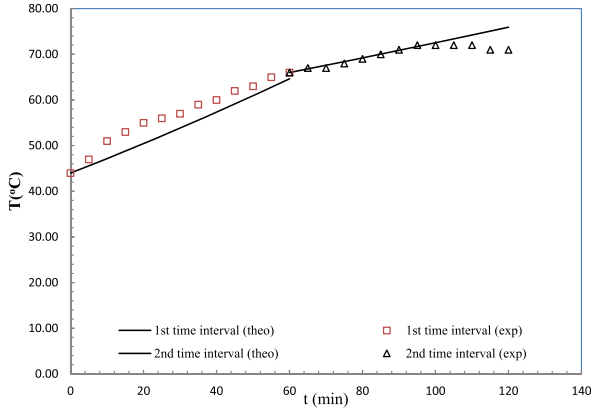

Fig. 23. The time variation of water temperature at an azimuth angle of 45° in two consecutive time intervals.

Another point that could be inferred by investigating the temperature variation at different azimuth angles is the highest rate of temperature inclination rate in azimuth angle of 30° compared to other cases; as could be seen in Table 4, the total temperature change through the experiment period for this case is 32.4 °C. The highest value of temperature change for the azimuth angle of 30° compared to other angles could be attributed to the latitude angle of the location; in other words, the highest solar absorbance for the heat pipe is for tilt angle and azimuth angles in the vicinity of latitude angle.

Another point that could be inferred by inspecting the figures is that in most cases, the measured water temperature is higher than the theoretical ones at positive angles (west direction) and in the first time interval; the average water temperature during the first and second time interval for different azimuth angles are shown in Table 5. This could be attributed to the effect of reflective radiation from

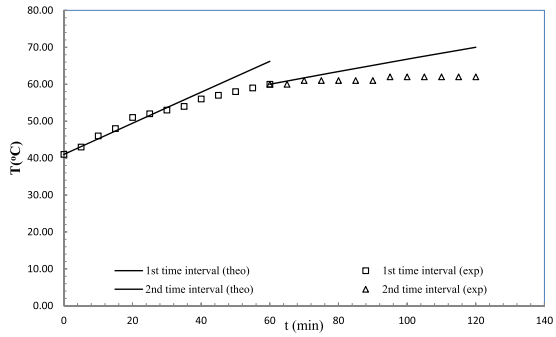

Fig. 24. The time variation of water temperature at azimuth angle of -45^{o} in two consecutive time intervals.

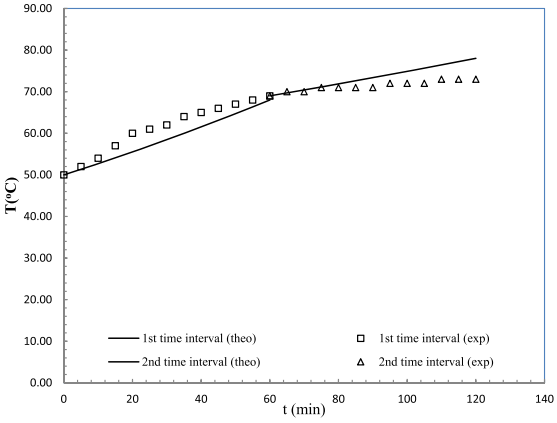

Fig. 25. The time variation of water temperature at azimuth angle of 60^{o} in two consecutive time intervals.

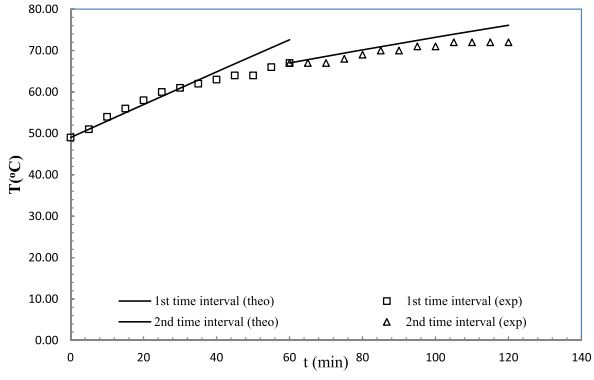

Fig. 26. The time variation of water temperature at azimuth angle of -60^{o} in two consecutive time intervals.

the ground surface which is the result of the close vicinity of the collector surface to the ground; during second-time interval and by increasing the water temperature this difference becomes less and the obtained temperatures via the experimental and theoretical approaches converge more.

4.3. The seasonal and yearly optimum tilt angle

After comparing the experimental and theoretical results and by approving the non-isotropic sky radiation as a reliable model for thermal performance prediction of heat pipe solar collectors, the optimum yearly and seasonal tilt angle of solar collectors was obtained at different latitudes angles located in the northern hemisphere and are listed in Table 6. The contents of this table were obtained using the subroutine written in Matlab software which takes the mean day of season, latitude angle of location and the sky clearance index (Table 1) as the inputs and gets the optimum tilt angle as the output.

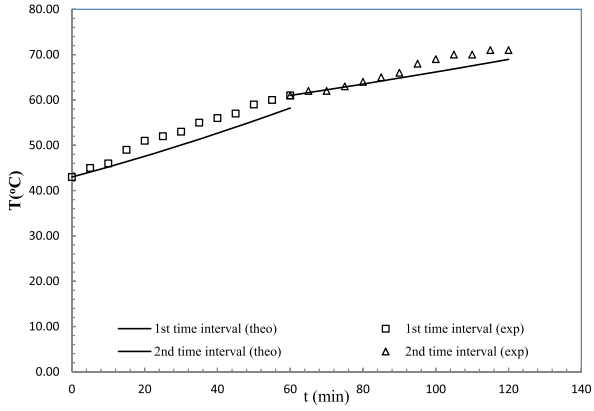

Fig. 27. The time variation of water temperature at an azimuth angle of 75° in two consecutive time intervals.

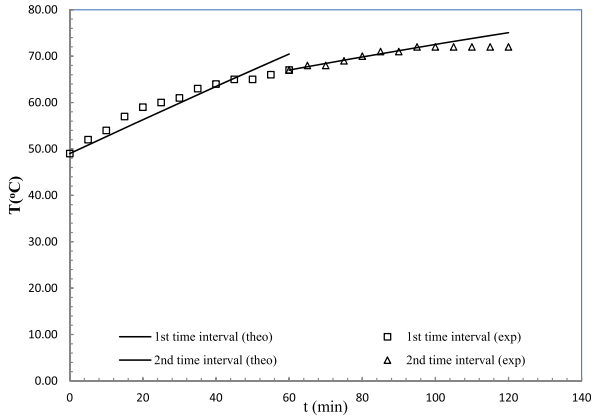

Fig. 28. The time variation of water temperature at azimuth angle of −75° in two consecutive time intervals.

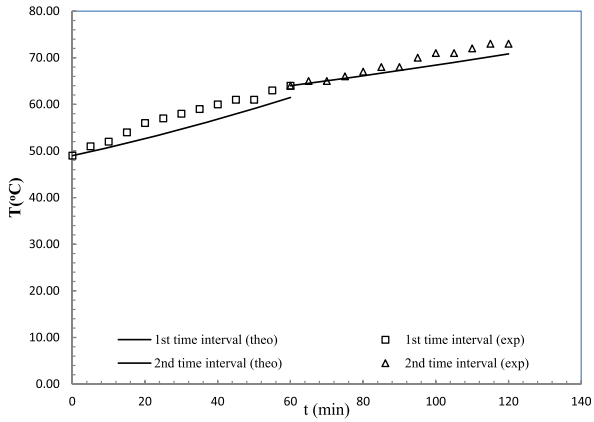

Fig. 29. The time variation of water temperature at azimuth angle of 90° in two consecutive time intervals.

The variation of optimum tilt angle vs the latitude angle in different seasons and throughout the year is depicted in Fig. 31. As could be seen the optimum tilt angle increased almost linearly by increasing the latitude angle; by increasing the latitude angle from 24° to 40°, the annual optimum tilt angle increased from 22° to 38°. Also, the optimum tilt angle is the highest for autumn and lowest for spring; this could be attributed to the highest and lowest inclination angle of the sun ray for these two seasons, respectively. The optimum tilt angle for each season and the whole year could also be correlated as the function of latitude angle as given by Eq. (15).

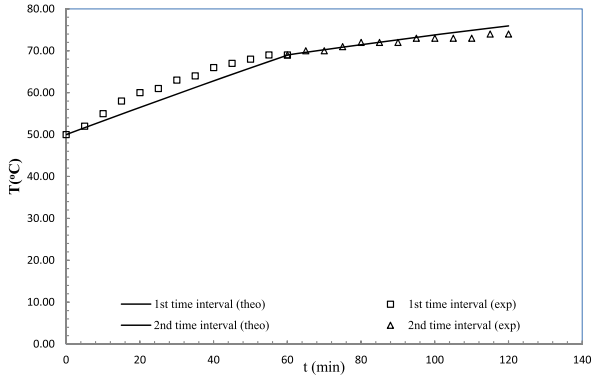

Fig. 30. The time variation of water temperature at an azimuth angle of -90^{o} in two consecutive time intervals.

Table 4
Percent change of measured water temperature during two-time intervals for different azimuth angles.

Angle%Change	15	−15	30	−30	45	−45	60	−60	75	−75	90	−90
1st interval	44	35	54	47	50	46	38	37	42	37	31	38
2nd interval	9.1	9.1	10.8	9.1	5.9	3.3	4.3	7.5	14.5	5.9	12.3	5.7
total	26.6	22.1	32.4	28.1	28.0	24.7	21.2	22.3	28.3	21.5	21.7	21.9

Table 5
The average water temperature during two-time intervals for different azimuth angles obtained by direct measurement and calculations.

	15	−15	30	−30	45	−45	60	−60	75	−75	90	−90
1st interval (theo)	57.2	61.1	52.2	58.0	54	53.6	58.7	60.9	50.3	59.8	54.9	59.6
1st interval (measu)	56.5	57.3	53.5	56.8	56.8	52.2	61.2	59.6	52.8	60.2	57.3	61.7
2nd interval (theo)	70.5	70.6	68.3	71.4	70.9	65.1	73.4	71.6	64.9	71.1	67.3	72.6
2nd interval (measu)	69.4	69.9	68.8	68.9	69.8	61.3	71.4	69.9	66.3	70.5	68.6	72

Table 6
The calculated optimum seasonal and yearly tilt angles for different northern latitudes of 24^{o} – $40.^{o}$

Latitude angle	Spring n = 135, $K_T = 0.53$	Summer n = 228, $K_T = 0.56$	Autumn n = 318, $K_T = 0.51$	Winter n = 47, $K_T = 0.51$	Yearly
24	5	11	40	34	22.5
26	7	13	42	36	24.5
28	9	15	44	38	26.5
30	10	17	46	40	28.25
32	12	19	48	42	30.25
34	14	21	50	44	32.25
36	16	23	52	46	34.25
38	18	25	54	48	36.25
40	20	27	56	50	38.25

$$\beta_{opt.} \approx \begin{cases} \varphi - 18 & spring \\ \varphi - 13 & summer \\ \varphi + 16 & autumn \\ \varphi + 10 & winter \\ \varphi - 1 & annual \end{cases} \tag{15}$$

The variation of hourly total solar heat flux vs the azimuth angles in four seasons was also calculated and its variation is depicted in Fig. 32. As shown, the highest value of incident radiation at each season took place at azimuth angle of zero which is toward the southern direction. Furthermore, the highest and lowest sensitivity of incident solar radiation to change of azimuth angle is at autumn and spring, respectively; by changing the direction collector surface from the west (90^{o}) or east (-90^{o}) to south (0^{o}), the incident solar heat flux changed by 38 % and 9 %, respectively. This could be attributed to more inclined solar radiation in autumn and less one in spring which brings about these two different behaviors.

This section could be concluded by this result that firstly the performance of the HP solar collectors is a strong function of tilt angle and relatively less dependent on the azimuth angle. By verifying the used model as the successful model for predicting thermal performance of HP collectors, the optimum tilt angle for different seasons could be chosen as given by Eq. (15).

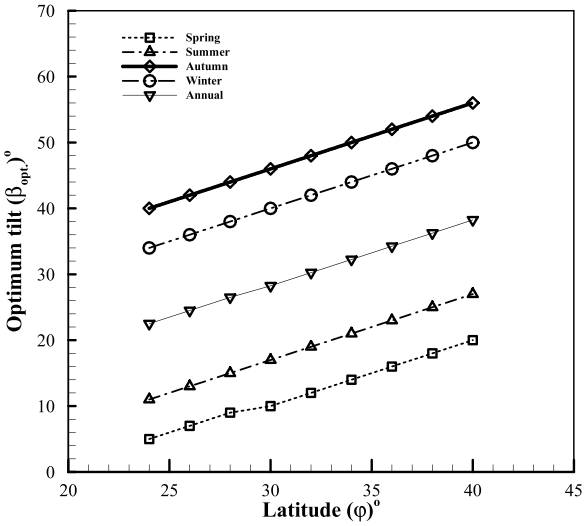

Fig. 31. The variation of optimum tilt angle vs the latitude angle for different seasons and throughout the year.

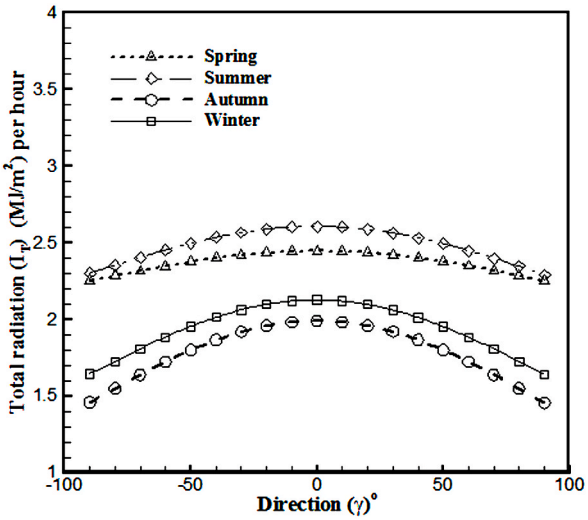

Fig. 32. The variation of hourly solar heat flux vs the azimuth angle.

5. Conclusion

Solar energy as a clean free source of energy, to be harvested effectively, requires the solar collector. The heat pipe solar collector with its large benefits over the other types draws large attention. The thermal performance of a solar heat pipe collector was studied via experimental and theoretical approaches. The performance of a heat pipe collector in different tilt and azimuth angles were investigated in location of the Isfahan city, Iran. The anisotropic sky model was selected as a theoretical model and the obtained experimental results were compared to theoretical ones. After approving the model, the optimum seasonal and yearly tilt angles were calculated and the correlation was also drawn. The finding could be used to improve the design of heat pipe solar collector and the proper orientation for the achievement of best performance. Also, for the conditions of present experimental study, which is in northern hemisphere, the correlation of optimum tilt and azimuth angle could be implemented. The obtained results could be summarized as follows.

- Despite the observed discrepancy between the water temperatures obtained by the experiment and theory, the same variation patterns of the two approaches show the good accuracy of the anisotropic sky model for estimating the thermal performance of heat pipe collectors.
- The lower water temperatures of the experimental than a theoretical approach could be attributed to tube heat loss to surroundings which has not been considered in calculations; also, the ground reflected coefficient makes some discrepancy. This case is seen at

higher-than-30° tilt angles and first-time intervals. The difference between theoretical and experimental results averaged between different tilt angles is 5 %.

- Through spring and summer, the optimum tilt angle is somewhat less and through autumn and winter the optimum tilt angle is beyond the latitude angle with the largest difference in spring and autumn. Also, for the whole year and under the conditions of the present study, the optimum tilt angle is nearly the same as the latitude angle of the location.
- The calculations show that under the conditions of the present study, the optimum zenith angle is toward the southern direction.
- For the future works, studying the effect of different orientation angles of HP collector on the influencing factors of natural convection inside the collector is recommended.

CRediT authorship contribution statement

Donghui Wei: Investigation, Writing – original draft. **Ali Basem:** Formal analysis, Writing – original draft. **As'ad Alizadeh:** Supervision, Writing – review & editing. **Dheyaa J. Jasim:** Investigation, Writing – original draft. **Haydar A.S. Aljaafari:** Validation, Methodology, Conceptualization, Data curation, Formal analysis. **Mohammadali Fazilati:** Formal analysis, Writing – review & editing. **Babak Mehmandoust:** Conceptualization, Data curation, Formal analysis. **Soheil Salahshour:** Methodology, Project administration.

Declaration of competing interest

The authors declare that they have no known competing financial interests or personal relationships that could have appeared to influence the work reported in this paper.

Data availability

No data was used for the research described in the article.

Acknowledgements

"Northeast Agricultural Scholar" academic backbone fund, Basic Research Support Program for Excellent Young Teachers in Heilongjiang Province.

References

[1] M. Sharmina, C. McGlade, P. Gilbert, A. Larkin, Global energy scenarios and their implications for future shipped trade, Mar. Pol. 84 (2017) 12–21.
[2] N. Alrikabi, Renewable energy types, J. Clean Energy Technol. 2 (2014) 61–64.
[3] M. Mozafarifard, A. Azimi, H. Sobhani, G.F. Smaisim, D. Toghraie, M. Rahmani, Numerical study of anomalous heat conduction in absorber plate of a solar collector using time-fractional single-phase-lag model, Case Stud. Therm. Eng. 34 (2022) 102071, https://doi.org/10.1016/j.csite.2022.102071.
[4] S. Dabiri, E. Khodabandeh, A.K. Poorfar, R. Mashayekhi, D. Toghraie, S.A. Abadian Zade, Parametric investigation of thermal characteristic in trapezoidal cavity receiver for a linear Fresnel solar collector concentrator, Energy (Oxford, England) 153 (2018) 17–26, https://doi.org/10.1016/j.energy.2018.04.025.
[5] Y. Shi, D. Toghraie, F. Nadi, et al., The effect of the pitch angle, two-axis tracking system, and wind velocity on the parabolic trough solar collector thermal performance, Environ. Dev. Sustain. 23 (2021) 17329–17348. https://doi.org/10.1007/s10668-021-01368-2.
[6] R. Shukla, K. Sumathy, P. Erickson, J. Gong, Recent advances in the solar water heating systems: a review, Renew. Sustain. Energy Rev. 19 (2013) 173–190.
[7] Y.F. Nassar, K.A. Amer, H.J. El-Khozondar, A.A. Ahmed, A. Alsharif, M.M. Khaleel, M. Elnaggar, R.J. El-Khozondar, A. Salem, Thermoelectrical analysis of a new hybrid PV-thermal flat plate solar collector, in: Proc. 2023 8th International Engineering Conference on Renewable Energy & Sustainability (ieCRES), IEEE, 2023, pp. 1–5.
[8] T. Zhang, W. Zheng, L. Wang, Z. Yan, M. Hu, Experimental study and numerical validation on the effect of inclination angle to the thermal performance of solar heat pipe photovoltaic/thermal system, Energy 223 (2021) 120020.
[9] A.A. Alammar, R.K. Al-Dadah, S.M. Mahmoud, Numerical investigation of effect of fill ratio and inclination angle on a thermosiphon heat pipe thermal performance, Appl. Therm. Eng. 108 (2016) 1055–1065.
[10] M. Elnaggar, Useful energy, economic and reduction of greenhouse gas emissions assessment of solar water heater and solar air heater for heating purposes in Gaza, Palestine, Heliyon 9 (6) (2023) 16803.
[11] M. Elnaggar, H. El-Khozondar, M. Bashir, W. Salah, Enhancing solar water heater system for utmost useful energy gain and reduction in greenhouse gas emissions in Gaza, Int. J. Environ. Sci. Technol. 20 (2023) 3749–3764.
[12] H. Mousazadeh, A. Keyhani, A. Javadi, H. Mobli, K. Abrinia, A. Sharifi, A review of principle and sun-tracking methods for maximizing solar systems output, Renew. Sustain. Energy Rev. 13 (2009) 1800–1818.
[13] S. Abdullah, The effect of using sun tracking systems on the voltage-current characteristics and power generation of flat plate photovoltaic, Energy Convers. Manag. 1 (2004) 1671–1679.
[14] T. Tomson, Discrete two-positional tracking of solar collectors, Renew. Energy 33 (2008) 400–405.
[15] M. Despotovic, V. Nedic, Comparison of optimum tilt angles of solar collectors determined at yearly, seasonal and monthly levels, Energy Convers. Manag. 97 (2015) 121–131.
[16] K. Skeiker, Optimum tilt angle and orientation for solar collectors in Syria, Energy Convers. Manag. 50 (2009) 2439–2448.
[17] H. Khorasanizadeh, K. Mohammadi, A. Mostafaeipour, Establishing a diffuse solar radiation model for determining the optimum tilt angle of solar surfaces in Tabass, Iran, Energy Convers. Manag. 78 (2014) 805–814.
[18] A. Sharma, M.A. Kallioğlu, A. Awasthi, R. Chauhan, G. Fekete, T. Singh, Correlation formulation for optimum tilt angle for maximizing the solar radiation on solar collector in the Western Himalayan region, Case Stud. Therm. Eng. 26 (2021) 101185.
[19] K. Chopra, V. Tyagi, A. Pandey, A. Sari, Global advancement on experimental and thermal analysis of evacuated tube collector with and without heat pipe systems and possible applications, Appl. Energy 228 (2018) 351–389.
[20] V. Kumar, S.V. Jain, Y. Shah, V.J. Lakhera, Parametric studies on interacting parameters influencing heat pipe performance, Proc. Inst. Mech. Eng. A J. Power Energy 235 (2021) 594–607.
[21] A.D. Hassan, R.A. Hussein, The variation effect of collector tilt angle on the heat pipe solar collector performance, Wasit J. Eng. Sci. 6 (2018) 21–27.
[22] M. Hu, R. Zheng, G. Pei, Y. Wang, J. Li, J. Ji, Experimental study of the effect of inclination angle on the thermal performance of heat pipe photovoltaic/thermal (PV/T) systems with wickless heat pipe and wire-meshed heat pipe, Appl. Therm. Eng. 106 (2016) 651–660.

[23] N. Nijegorodov, K. Devan, P. Jain, S. Carlsson, Atmospheric transmittance models and an analytical method to predict the optimum slope of an absorber plate, variously oriented at any latitude, Renew. Energy 4 (1994) 529–543.
[24] S. Soulayman, W. Sabbagh, Solar collector optimum tilt and orientation, Open J. Renew. Sustain. Energy 2 (2015) 1–9.
[25] A. Beckman William, Solar Engineering of Thermal Processes, A Wiley-Interscience Publication, JOHN WİLEY& SONS, INC, Canada, 1991, p. 888.
[26] H. Heywood, Operating experiences with solar water heating, IHVE J. 39 (1971).
[27] P.J. Lunde, Solar Thermal Engineering: Space Heating and Hot Water Systems, 1980.
[28] A. El-Sebaii, F. Al-Hazmi, A. Al-Ghamdi, S.J. Yaghmour, Global, direct and diffuse solar radiation on horizontal and tilted surfaces in Jeddah, Saudi Arabia, Appl. Energy 87 (2010) 568–576.
[29] A.M. Noorian, I. Moradi, G.A. Kamali, Evaluation of 12 models to estimate hourly diffuse irradiation on inclined surfaces, Renew. Energy 33 (2008) 1406–1412.
[30] H. Yazdanpanah, R. Mirmojarabian, H. Barghi, Estimation of solar global radiation on horizontal surface in isfahan, J. Geogr. Environ. Plan. (Persian) 37 (2010) 95–104.
[31] H. Yazdanpanah, H. Barghi, R. Mirmojarabian, H. Barghi, Estimating total incoming solar radiation on the earth surface of Isfahan, Geogr. Environ. Plan. 21 (2010) 95–104.
[32] S.Y. Alsadi, Y.F. Nassar, Estimation of solar irradiance on solar fields: an analytical approach and experimental results, IEEE Trans. Sustain. Energy 8 (2017) 1601–1608.
[33] T. Erb, U. Zhokhavets, G. Gobsch, S. Raleva, B. Stühn, P. Schilinsky, C. Waldauf, C.J. Brabec, Correlation between structural and optical properties of composite polymer/fullerene films for organic solar cells, Adv. Funct. Mater. 15 (2005) 1193–1196.
[34] S.M. Van Genugten, Italian and British Relations with Libya Pride and Privileges 1911–2011, The Johns Hopkins University, 2012.
[35] Y. Nassar, Solar Energy Engineering [active Application] in Arabic Language, 2006.
[36] K. Bakouri, T. Foqha, O. Ahwidi, A. Abubaker, Y. Nassar, H. El-Khozondar, Learning lessons from Murzuq-Libya meteorological station: evaluation criteria and improvement recommendations, J. Solar Energy Sustain. Dev. 12 (2023).